Journal of *Marine Science and Engineering*

MDPI

Article

Antioxidant and Anti-Breast Cancer Properties of Hyaluronidase from Marine *Staphylococcus aureus* (CASMTK1)

Kathiravan Thirumurthy [1,2], Kalidasan Kaliyamoorthy [3,*], Kathiresan Kandasamy [2], Mohanchander Ponnuvel [4], Voranop Viyakarn [3], Suchana Chavanich [3] and Laurent Dufossé [5,6,*]

1 Department of Microbiology, Tagore College of Arts and Science, Chromepet, Chennai 600044, India
2 Faculty of Marine Sciences, Annamalai University, Parangipettai 608502, India
3 Reef Biology Research Group, Department of Marine Science, Faculty of Science, Chulalongkorn University, Bangkok 10330, Thailand
4 Department of Zoology, Madras Christian College (Autonomous), East Tambaram, Chennai 600059, India
5 Chemistry and Biotechnology of Natural Products, CHEMBIOPRO, Université de La Réunion, ESIROI Agroalimentaire, 15 Avenue René Cassin, CS 92003, CEDEX 9, 97744 Saint-Denis, France
6 Laboratoire ANTiOX, Université de Bretagne Occidentale, Créac'h Gwen, 29000 Quimper, France
* Correspondence: marinedasan87@gmail.com (K.K.); laurent.dufosse@univ-reunion.fr (L.D.); Tel.: +91-99-6526-2514 (K.K.); +262-692-402-400 (L.D.)

Abstract: This work studied the antioxidant and anti-breast cancer properties of hyaluronidase, extracted from a potential marine strain, *Staphylococcus aureus* (CASMTK1), isolated from Parangipettai coastal waters in southeast coast of India. The Staphylococcal enzyme production was tested under different carbon and nitrogen sources; and recorded the maximum production when the microbial strain was cultured with starch as the carbon source and ammonium sulphate as the inorganic nitrogen source with the enzyme production of 92.5 U/mL and 95.0 U/mL, respectively. The hyaluronidase enzyme production was also tested in different pH and temperature; and recorded the maximum yield of 102.5 U/mL in pH 5 and that of 95.5 U/mL in 45 °C. The partially purified enzyme was subjected to FTIR and FT Raman technique and found the presence of the amide- I and II, Carboxyl, N-H bending, C-H stretching and α-helices and β-sheet proteins between wave number 1500–1700 cm^{-1}. The partially purified enzyme also exhibited strong antioxidant and in-vitro breast cancer properties. The enzyme showed the highest hydroxyl radical scavenging activity of 79% at the 50 µg/mL concentration, and this activity increased in a dose-dependent manner. The enzyme inhibited proliferation of the breast cancer cell line of MCF-7, and it caused 100% cell death at the concentration of 80 µg/mL. The enzyme generated capacity of producing free radicles that damage the cancer cells, and this effect was very nearer to the standard drug, paclitaxel. The enzyme damaged the cancer cells and induced apoptosis in 78% of cancer cells as evident by condensed or fragmented chromatin at 40 µg/mL. Further purification of the enzyme, analysis of its molecular aspects, and elucidation of exact mechanisms of its biological activities will throw new light on the utility of staphylococcal hyaluronidase in anticancer chemotherapy.

Keywords: marine bacteria; *Staphylococcus* sp.; hyaluronidase; antioxidant; anti-breast cancer activity

Citation: Thirumurthy, K.; Kaliyamoorthy, K.; Kandasamy, K.; Ponnuvel, M.; Viyakarn, V.; Chavanich, S.; Dufossé, L. Antioxidant and Anti-Breast Cancer Properties of Hyaluronidase from Marine *Staphylococcus aureus* (CASMTK1). *J. Mar. Sci. Eng.* **2023**, *11*, 778. https://doi.org/10.3390/jmse11040778

Academic Editor: Azizur Rahman

Received: 11 March 2023
Revised: 30 March 2023
Accepted: 31 March 2023
Published: 3 April 2023

1. Introduction

Cancer is a large group of diseases that can begin in almost any organ or tissue of the body when abnormal cells grow uncontrollably, invade neighboring parts of the body, and/or spread to other organs [1]. Cancer is the world's second leading cause of death [2], accounting for an estimated 9.6 million deaths, or one out of every six deaths in 2018 [1]. Cancer is caused by a small number of inherited or environmental-induced genetic mutations [3]. The most prevalent cancers in men are lung, prostate, colorectal, stomach, and liver cancers, whereas the most prevalent cancers in women are breast, colorectal, lung, cervical, and thyroid cancers [1,4].

Breast cancer is one of the most predominant cancers in women, and the second most common type of cancer overall, after lung cancer [2,5]. Breast cancer starts in the lobules, which are milk-producing glands in the breast tissue, and the ducts that connect the lobules to the nipple. A number of breast cancers are known, and they are contained within the ducts (ductal carcinoma in situ, or DCIS), or lobules (lobular carcinoma in situ, or LCIS); DCIS is the most common, accounting for 83% of cases, whereas LCIS accounts for 11% of cases in females, found between 2004 and 2008. The breast tumors are invasive or infiltrating. On a molecular level, it is a diverse disease that most frequently affects women [6].

In general, eliminating the tumor and preventing metastasis and recurrence are the main goals of breast cancer treatment. In more than 94% of patients with breast cancer, there were no identifiable metastases at the time of diagnosis. The local treatment for non-metastatic breast cancer entails surgical resection, sampling or removal of axillary lymph nodes, preoperative and postoperative radiotherapy, or both. The same primary systemic treatment is utilized in the cases of metastatic breast cancer, including neoadjuvant, adjuvant, cytotoxic, and co-administered medications as well as surgery and radiotherapy, which are exclusively used for palliative care. The main objectives in this case are symptom relief and life extension [7].

Generally, drugs are cured collectively, with surgical procedure, radiation and biotherapy being the most important techniques in the treatment of most cancers. Chemotherapy, which is a method of using chemical medications to either kill tumor cells or stop them from growing and proliferating, was once the only kind of cancer drug treatment [8]. Chemotherapy's biggest flaw is its significant side effects and toxicity. Most cancers have been treated in the past 20 years with a first-rate shift from broad-spectrum cytotoxic medications to targeted drugs [9]. Targeted medications are more effective and have lower side effects than conventional chemotherapy drugs because they can specifically target most cancer cells while sparing normal cells. Estrogen receptors alpha and beta (ER-alpha and ER-beta) being present or absent is a crucial aspect of breast cancer. Estrogens are a class of hormones that are active and play a major role in cancer progression, cell division, and proliferation [10,11].

The number of targeted cancer treatments approved by the FDA during the past 20 years has dramatically increased [12]. However, the majority of medications have adverse effects. Tamoxifen is a prodrug that uses the estrogen receptor to partially prevent the uptake of estrogen (ER) [13]. According to prior research, tamoxifen can reduce the chance of ER^+ breast cancer recurrence by half [14]. However, tamoxifen has known adverse effects and has been linked to a number of other health hazards, including endometrial cancer, blood clots, and paralysis [15]. Medical treatments for breast cancer include aromatase inhibitors. It works to suppress the conversion of androgens to estrogens in postmenopausal women, preventing them from producing estrogen, leading to estrogen depletion [16]. Taxanes are cytotoxic chemotherapy drugs that disrupt the structure and function of microtubules by acting as mitotic inhibitors. The most common form of neoadjuvant chemotherapy for breast cancer is still a combination of taxanes and anthracyclines. Early breast cancer patients have a higher chance of surviving when a taxane medication is added to popular chemotherapy. However, using taxanes increases the likelihood of some side effects, including febrile neutropenia and neuropathy [17]. Cisplatin, carboplatin, and oxaliplatin are among the anticancer medications in the platinum (Pt)-based pharmacological class. They are effective against a wide range of tumors, as well as lung, bladder, colon, testicular, ovarian, and breast cancers. However, the severe dose-limiting side effects of these drugs limit their use. especially myelosuppression for carboplatin, nephrotoxicity for cisplatin, and neurotoxicity for oxaliplatin [18].

Antioxidants play vital roles in the upkeep of cell integrity and accordingly are imperative in keeping the homeostasis of the host immune system. The stability between the ranges of pro-oxidants and antioxidants defines the cell destiny of genomic integrity by means of retaining the redox reputation of the cells [19]. These antioxidants protect against

cell damage by reacting and eliminating oxidizing free radicals, which find relevance in adjuvant chemotherapy. The free radicals such as superoxide anion, hydroxyl radical, hydrogen peroxide and nitric oxide (Commonly known as ROS) are known to damage the cells, by reacting with unsaturated fatty acids in the plasma membranes, which lead to reductions in membrane fluidity, and to damage membrane proteins [20]. These effects are blocked by the use of antioxidants, which are present in natural medicines to treat cancers, cardiovascular illnesses neurodegenerative illnesses, Parkinson's, and Alzheimer's desease [21].

The coronavirus pandemic (COVID-19) in 2020 had a negative impact on cancer detection and therapy [2]. This necessitates to find new potent drug from natural sources. Marine organism has been recognized as a repository of structurally novel secondary metabolites, some of which have beneficial biological activities and recently numerous novel bioactive compounds have been isolated from these microorganisms and only a few of them are under investigation for development as new drugs [22].

Hyaluronidase is an enzyme that breaks down the mucopolysaccharide hyaluronic acid, and it has long been utilized to improve drug absorption into tissue and lessen tissue damage in situations where a drug has extravasated. As a part of the muco-protein ground substance or tissue cement, the enzyme raises membrane permeability, lowers viscosity, and facilitates tissue permeation [23]. The enzyme is mostly found in Gram-positive bacteria belonging to the genera of *Streptococcus*, *Staphylococcus*, *Propionibacterium*, *Peptostreptococcus* and *Streptomyces*, and these microbes play vital role on ecological balance in the marine environment [24]. The hyaluronidase enzyme (HE) is known for its clinical importance in orthopaedic, surgery, ophthalmology, internal medicine, cardiology, dermatology, gynaecology, and anticancer treatments [23]. Hyaluronidase is sometimes injected with chemotherapy drugs to help the medicine to penetrate deeper into brain tumors [25]. Hyaluronidase is used in medicine to improve the tissue absorption of several medicines. This enzyme can facilitate drug diffusion into the extracellular matrix and raise blood vessel permeability. In practice, the sub-ministration of the enzyme could avoid tissue injury after extravasation of a number of drugs, including parental nourishment solution, electrolyte infusions, antibiotics, aminophylline, and chemotherapy drugs, and lowering their concentration [26]. The marine-derived hyaluronidase enzyme has not been extensively studied for its bioactive potential. In view of the above facts, the present work was undertaken to study hyaluronidase from marine *Staphylococcus* species for its antioxidant and anti-breast cancer properties.

2. Materials and Methods

2.1. Sample Collection and Isolation of Staphylococcus Species

In totals, five stations were selected from the inshore waters of Parangipettai, located in southeast coast of India: Station I (11°30′29″ N and 79°49′15″ E), Station II (11°28′33″ N and 79°49′44″ E), Station III (11°26′40″ N and 79°50′13″ E), Station IV (11°24′35″ N and 79°50′58″ E), Station V (11°22′25″ N and 79°51′36″ E). The surface marine water samples were collected in 100 mL sterile screw capped bottles, transported to the laboratory in a portable ice box, and analysed instantly for bacteriological examination. The membrane filtration technique was used to inoculate samples on the selective culture media. A 10-fold dilution of each sample was prepared in 10 mL sterile Phosphate-buffer saline. Each sample was filtered over a 0.45 µm filter papers. Then, the filter paper was placed by impregnation of the filtered surface over the mannitol salt agar selective medium (MSA) for the selective isolation of *Staphylococcus* species. Triplicates were maintained for each sample. The inoculated petri plates were incubated at 37 °C for 24 h. After incubation, bacterial colonies were counted using a colony counter chamber and calculated for colony forming units (CFU) per/mL. The isolated colonies were sub-cultured using the MSA medium for further studies.

2.2. Morphological and Molecular Identification of Staphylococcus Species

Based on morphological, physiological, and biochemical characteristics, the microbial colonies were examined for the presence of *Staphylococcus* species using the procedure described in Bergey's determinative bacteriology handbook [27] and also based on molecular characteristics by extracting genomic DNA and amplifying PCR products [28].

2.3. Sequencing and Phylogenetic Analysis of 16S rDNA Gene

The amplicons were directly sequenced using a 373A model sequencer and the PRISM Ready Reaction Dye Deoxy Terminator Cycle sequencing kit. The results were converted into sequence information with the help of William Pearson's lalign programme (http://www.ch.embnet.org/software/lalignform.html, access on 10 October 2023), and the partial sequences were combined into a single sequence using the results. The partial sequences were processed into sequence information with a sequence analysis chromas software (version 2.33; Technelysium Pvt., Ltd., Brisbane, QLD, Australia; http://www.technelysium.com.au/chromas.html, access on 17 September 2014). The isolates were found using a single sequence analysis of the generated data that was dynamited through the NCBI database. In order to find the closest neighbours to the cloned sequences, a BLAST search of the National Center for Biotechnological Information (NCBI) was conducted after the sequences were modified using Vecscreen. The Ribosomal Database Plan (RDP) classifier tool was used to carry out taxonomic assignments (http://rdp.cme.msu.edu/, access on 17 September 2014). The greatest likelihood approach was used to infer a phylogenetic tree. MEGA 6.0 software was used to run the tree-creating algorithm and analysis [29].

2.4. Enzyme Assay

The growth of the CASMTK1 strain was determined using a UV-Visible spectrophotometer at 675 nm in mannitol salt broth (MSB) incubated at 37 °C on a rotating shaker at 150 rpm for 24 h. The 24 h grown bacterial broth was centrifuged at 14,000 rpm for 10 min, and the supernatant was analyzed by turbidity reduction by measuring the absorbance at 600 nm to check the hyaluronidase activity [30].

2.5. Optimization of Staphylococcal Hyaluronidase

2.5.1. Effect of Salinity

The suitable salinity of the culture medium to support maximum enzyme production was determined by maintaining the cultures with varying salinity at 25, 30, 35, 40 and 45 PSU.

2.5.2. Effect of pH

The optimum pH of the culture medium to support maximum enzyme production was determined by maintaining the cultures with varying pH of 4, 5, 6, 7 and 8.

2.5.3. Effect of Temperature

The appropriate temperature of the culture medium to support maximum enzyme production was determined by keeping the cultures with varying temperatures of 25 °C, 35 °C, 40 °C, 45 °C and 50 °C.

2.5.4. Effect of Incubation Period

The optimal incubation period of the culture medium to support maximum enzyme production was determined by keeping the cultures with varying periods of 24, 48, 72, 96 and 120 h.

2.5.5. Effect of Carbon Sources

The suitable carbon source of the culture medium to support maximum enzyme production was determined by keeping the cultures with five different sources of carbon

(maltose, fructose, lactose, starch, and cellulose) each at a concentration of 4% (w/v) to the basal medium.

2.5.6. Effect of Inorganic Nitrogen Sources

The suitable nitrogen source of the culture medium to support maximum enzyme production was determined by keeping the cultures with five different sources of nitrogen (ammonium acetate, ammonium nitrate, ammonium sulphate, sodium nitrite, and urea) each at a concentration of 0.5% (w/v) to the basal medium.

2.6. Purification of Staphylococcal Hyaluronidase

The Staphylococcal hyaluronidase was partially purified from the supernatant of CASMTK1 culture incorporated with 25 µL of hyaluronic acid as the substrate maintained at 37 °C on a rotating shaker at 150 rpm for 48 h. The supernatant was subjected to partial purification by ammonium sulfate precipitation, gel filtration and ion exchange chromatography [31]. Molecular weight of the partial purified enzyme was determined using SDS-PAGE.

2.7. FT-IR and FT-R Spectro Photometry Data Analysis

The Staphylococcal hyaluronidase was dissolved in D_2O with guanidine hydrochloride (Gdn HCl) for measurements of FT-IR spectra (Fourier Transform- Infrared) using an infrared spectrophotometer (NEXUS 670, Thermo Nicolet) through 64 times of scanning [32]. Using the BRUKER RFS 27 and Fourier Transform-Raman (FT-R) spectrometer, which are available at the high-end analytical instrument facilities in Indian Institute of Technology, Chennai, India, a FT-R spectrum was acquired in the range of 500–3000 cm^{-1}. The spectra were examined with the aid of the program ORIGIN 6.0.

2.8. Antioxidant Properties of Staphylococcal Hyaluronidase

Staphylococcal hyaluronidase was tested in different concentrations of 10, 20, 30, 40 and 50 µg/mL for antioxidant properties by following five assay methods for Total reducing power [33], DPPH radical scavenging [34], Total antioxidant [35], Superoxide scavenging [36], Hydroxyl radical scavenging [37] using L-ascorbic acid as a positive control.

2.9. Measurement of Cell Proliferation by MTT Cytotoxicity Assay

The human breast cancer (MCF-7) cell line was obtained from the National Center for Cell Science (NCCS) in Pune, India. The MCF-7 cells were treated with Staphylococcal hyaluronidase and the standard drug, Paclitaxel in different concentrations (10–100 µg/mL) and incubated at 37 °C in 5% CO_2 incubator for 24 h. Cytotoxicity in terms of IC_{50} was determined by analysing 3-4,5-dimethyl-2,5-biphenyl tetrazolium bromide (MTT, Sigma Chemical Co., St. Louis, MO, USA) and measured by the reduction of MTT at 540 nm by using a spectrophotometer [38].

2.10. Measurement of Intracellular Reactive Oxygen Species (ROS) in MCF-7 Cells

A non-fluorescent probe called 2, 7-diacetyl dichlorofluorescein diacetate (DCFH-DA), which may grow into extracellular matrix of cells and be oxidised by ROS to fluorescent dichlorofluorescein, was used to evaluate the ROS level caused by hyaluronidase in the MCF-7 cell line. In a spectrofluorimeter, the non-fluorescent DCFH-DA and highly fluorescent DCF were detected at emission filters set at 485 ± 10 nm and 530 ± 12.5 nm, respectively [39].

2.11. Apoptotic Changes by Acridine Orange/Ethidium Bromide Dual Staining Method

Apoptosis induced by hyaluronidase and paclitaxel treated and untreated cells (2×10^4/well), seeded into 6- micro well plate and incubated in a CO_2 incubator for 24 h, was observed for the apoptotic morphology changes (nuclear condensation and

segmentation) by staining with AO/Ebr and observing under a fluorescence microscope with blue filter [40].

2.12. Statistical Analysis

SPSS-16 was used to perform the ANOVA and Duncan's Multiple Range Test (DMRT) statistical analyses. The values are given as means ± S.D for each group. $p \leq 0.05$ was considered as level of significance.

3. Results

3.1. Morphological and Molecular Identification of Staphylococcus sp. CASMTK1

In total, 60 bacterial strains were isolated from five sampling locations of Parangipettai coastal waters. Based on survival, morphological, biochemical and microscopical characters the predominant 12 isolates (CASMTK1-CASMTKK12) were identified belonging to the genus Staphylococcus. All of these strains were screened for enzyme production. The CASMTK1 strain was found to be the most potent for the enzyme production. The strain was found to be Gram positive cocci of about 0.5 to 1.0 µm in diameter, arranged in irregular grape like clusters, pairs and occasionally in short chains. The morphology of the colony was a large circle, convex, smooth, shiny, opaque, and easily emulsifiable. Mannitol salt agar (MSA) a selective medium was used for isolating Staphylococcus sp., which could ferment mannitol of the medium to produce yellow colonies (Figure 1).

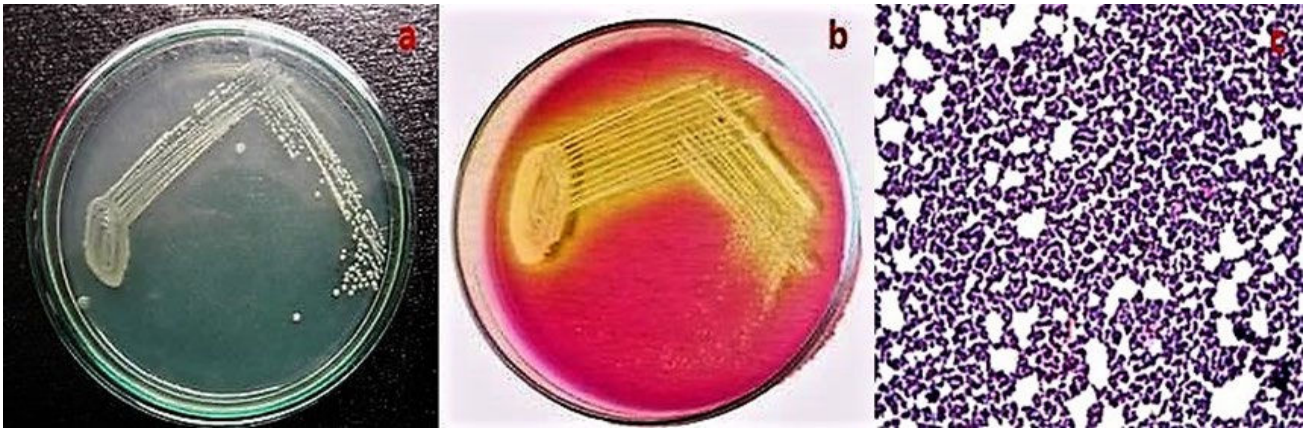

Figure 1. Morphological and microscopical view of CASMTK1 on (**a**). Nutrient agar, (**b**). Mannitol salt agar, (**c**). Gram's staining clusters of the *Staphylococcus* sp., under light microscope. Cultural Characteristics: They are aerobes and facultative anaerobes. Optimum temperature for growth is 37 °C range being 12–44 °C. Optimum pH is 7.5. (**a**) Nutrient agar: After overnight incubation at 37 °C colonies are 1–2 mm in diameter with a smooth glistering surface. They are opaque and easily emulsifiable. Most of the strains produce non diffusible golden yellow carotene pigment, though some strains are white colonies, (**b**) Mannitol salt agar: 1% mannitol, 7.5% sodium chloride and 0.0025% phenol red are added to nutrient agar. This is both selective and indicator medium. Most strains of *S. aureus* ferment mannitol therefore, due to the production of acids their colonies are surrounded by yellow zones. Otherwise, the colonies resemble those seen on nutrient agar, (**c**) Gram's staining: *Staphylococci* are Gram positive cocci about 0.5–1.0 µm in diameter. They are arranged in irregular grape like clusters, pairs and occasionally in short chains.

Furthermore, the 16S region of rRNA from the strain (CASMTK1) was sequenced. According to NCBI BLAST analysis, the marine strain of *Staphylococcus* sp. (CASMTK1) (Accession No. JX435813) was found 98.40% closer to *Staphylococcus aureus* RA 20 (AB634830). The phylogenetic analyses also confirmed the taxonomic position of the strain (Figure 2). The evolutionary history was inferred by utilizing the greatest likelihood method. The tree with the highest log probability (−3661.8091) is shown. The percentage of trees, in which the associated tax is aggregated is shown beside the branches. The initial trees for the

heuristic search were obtained by applying the Neighbor-Joining method to a matrix of estimated pairwise distances using the Maximum Composite Likelihood Approach (MCLA). The tree is constructed according to scale, and the length of the branches is measured by the number of substitutions per site. There were 934 positions in total in the final dataset.

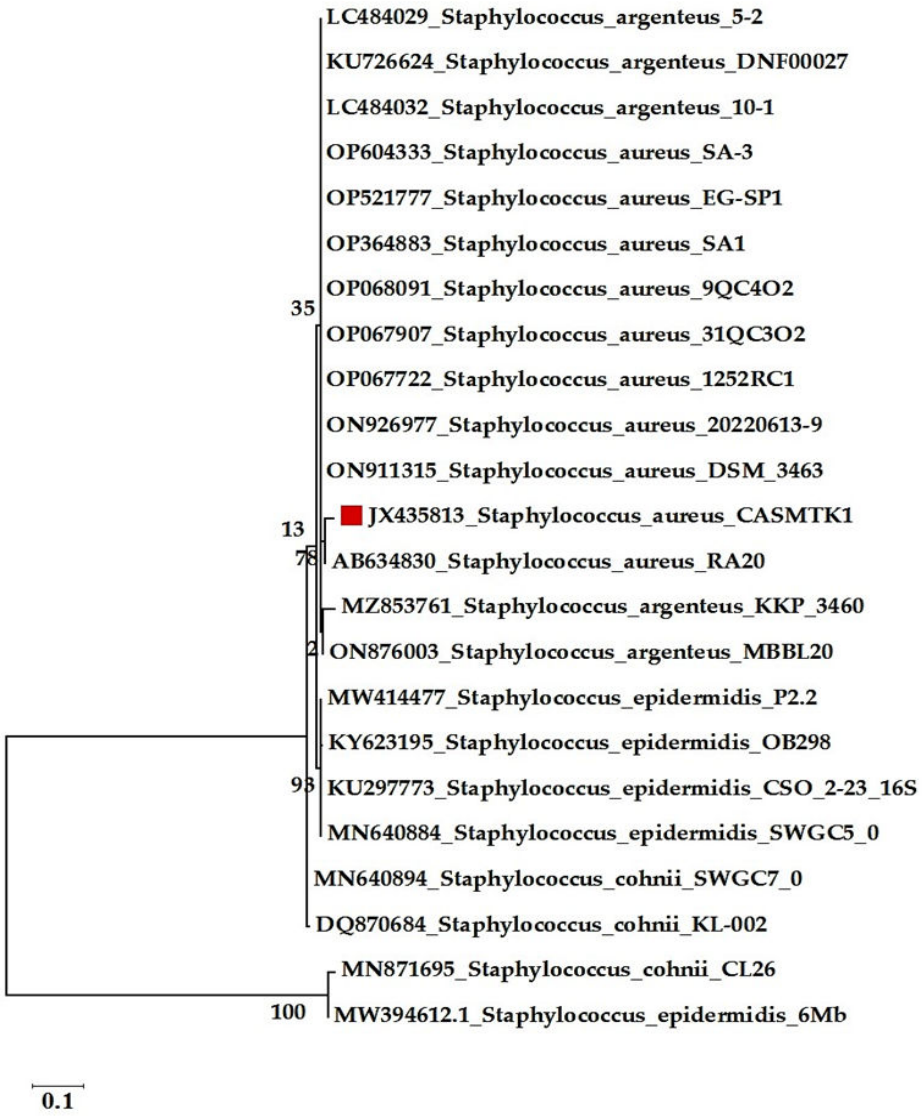

Figure 2. Maximum Likelihood phylogenetic tree analysis of CSMTK1 with 16S rRNA gene sequence and values are expressed as percentage of 1000 replications as shown at the branch points (red square = this study organism).

3.2. Enzyme Assay and Molecular Weight Analysis Using SDS- PAGE

CASMTK1 cell growth phase was determined by measuring with UV-Visible spectrophotometer (OD) at 675 nm using a spectrophotometer (Figure 3). The highest growth rate of 1.01 OD at 675 was achieved by 12 h for log phase during on batch culture (Figure 3b).

CF- Control fraction, the protein produced after application of enzymatic stages under optimum for maximum enzymatic production.

Table 1 shows enzyme activity, pH values and times used in the turbidity test are summarized. The activity of partially purified staphylococcal hyaluronidase used in the turbidity assay is expressed in terms of units (1 unit (U) of hyaluronidase catalyses the liberation of 1 μmol N-acetyl-D-glucosamine (NAG) at the reducing ends of sugars per minute). The enzyme activity was positive from the formation of the red-coloured

product per unit time, utilizing standards with known NAG concentration as tested by the turbidimetric assay.

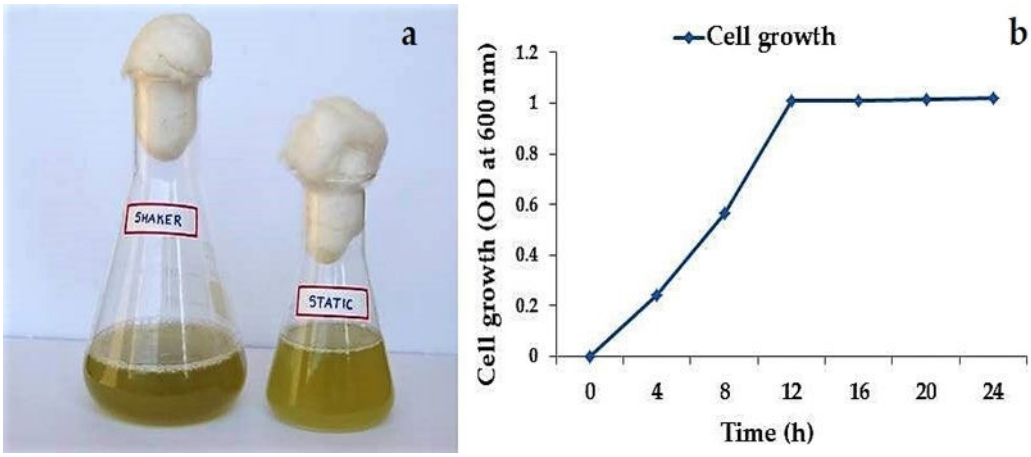

Figure 3. (**a**) Enzyme production and (**b**) cell growth characteristics of *S. aureus* CASMTK1. Effect of enzyme production based on incubation period in 100 mL of the modified Mannitol salt broth, placed in the 250 mL sterile flask and added with 25 µL of hyaluronic acid in the medium. After sterilization by autoclaving, the flasks were cooled and inoculated with 5% *v*/*v* inoculum and incubated at 37 °C on a rotary shaker at 150 rpm for 24 h and bacterial cell growth was observed.

Table 1. Enzymatic activities of staphylococcal hyaluronidase turbidity assay.

Enzyme	Enzyme Solution Prepared (mU/mL)	Enzyme Solution to Add Incubated Samples (µL)	Enzymatic Activity in Incubated Samples (mU)	pH	Incubation Time (h)
Staphylococcal hyaluronidase	20	10	0.22	5	0.3
Streptomyces hyaluronidase	20	10	0.21	5	0.3
Bovine testicular hyaluronidase	9.0	30	0.27	5	0.5

Fractioned precipitation with ammonium sulphate attained a specific activity of 198.12 U/mL at 80–90% saturation (Table 2). The recovered protein was 4.12 mg in precipitated fraction and 32.22 mg in partially purified fraction. The specific activity of the hyaluronidase enzyme was 33.26% in ammonium sulphate precipitation, 24.12% in ion exchange chromatography and 18.36% in gel filtration chromatography. The molecular weight of the partially purified enzyme was found to be 92 kDa by comparing the protein marker, Phosphorylase B on 12% SDS-PAGE gel electrophoresis (Figure 4). The specific activity of the Staphylococcal hyaluronidase enzyme was 90% and the total yield was at 18.36%.

Table 2. Fractionated precipitation marine *Staphylococcus aureus* CASMTK1 hyaluronidase with ammonium sulphate.

$NH4_2$ (SO_4) Saturation (%)	Protein Content (mg)	Total Activity (U/mL)	Specific Activity (U/mL/Protein)	Recovered Protein Activity (%)	Recovered Protein Activity (%)	Purification Fold
CF	254	593	2.33	100	100	1
0–10	56.2	18.76	0.36	22.66	4	0.14
10–20	49	11.22	0.24	19.18	2.01	0.12
20–30	36	34.26	0.85	14.66	6.02	0.6
30–40	28.1	14.14	0.62	11.22	3.01	0.26
40–50	23	14.74	0.78	9.46	3.04	0.32
50–60	19.2	11.36	0.64	7.2	2.01	0.29
60–70	19	12.18	0.69	7.16	2.05	0.3
70–80	13.14	48.62	4.12	4.82	9.12	1.82
80–90	10.12	198.12	19.26	4.12	33.26	9.12
Total	253.76	363.40	27.56	93.32	64.52	

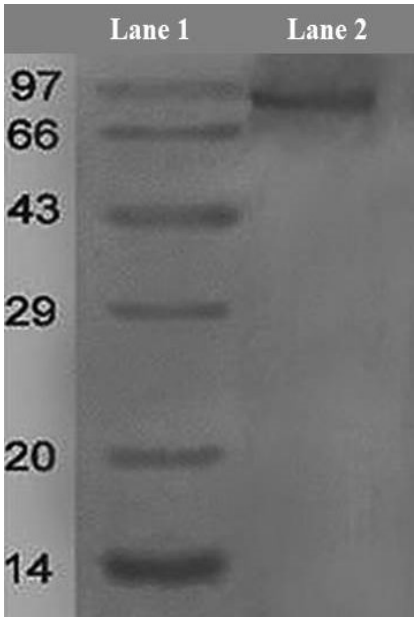

Figure 4. Molecular weight determination of partially purified Staphylococcal hyaluronidase enzymes by SDS-PAGE analysis Lane 1: molecular weight standard protein; Lane 2: Staphylococcal hyaluronidase resulted from purification.

3.3. Optimization of Staphylococcal Hyaluronidase Production from Marine S. aureus

The optimization of Staphylococcal hyaluronidase production from marine *S. aureus* is given in Supplementary Table S1. The maximum amount of hyaluronidase production was found at pH 5 (102.5 U/mL), followed by pH 4 (93.0 U/mL), pH 6 (80 U/mL), pH 7 (72.5 U/mL), while the minimum level of production was observed at pH 8 (65.0 U/mL) (Figure 5c); at 40 °C (95.5 U/mL), followed by 35 °C (86.8 U/mL), 45 °C (81.3 U/mL), 30 °C (71.6 U/mL), and 25 °C (63.2 U/mL) (Figure 5d). The highest amount of hyaluronidase production was observed at 35 PSU (91.3 U/mL), followed by PSU 40 (86.1 U/mL), PSU 30 (78.4 U/mL), PSU 25 (62.8 U/mL), whereas the lowest level of production was observed at PSU 45 (54.6 U/mL) (Figure 5e). The maximum hyaluronidase production was observed at 96 h (98.1 U/mL), followed by 72 h (84.6 U/mL), 120 h (83.9 U/mL), 48 h (69.3 U/mL), while the minimum level of production was observed at 24 h (63.2 U/mL) (Figure 5f). Regarding carbon sources, the highest hyaluronidase production was found in starch (92.5 U/mL), followed by fructose (82.5 U/mL), maltose (77.5 U/mL), lactose (60 U/mL), while the lowest production was recorded in cellulose (52.5 U/mL) (Figure 5a). Regarding inorganic nitrogen sources, the maximum production of hyaluronidase was observed in ammonium sulphate (95 U/mL), followed by ammonium nitrate (62.5 U/mL), sodium nitrate (57.5 U/mL), and urea (87.0 U/mL), whereas the minimum level of production was noted in ammonium acetate (35 U/mL) (Figure 5b).

3.4. FT-IR and FT-R Spectroscopy Studies of Staphylococcal Hyaluronidase

A fast and inexpensive way to characterize the properties of chemicals and to identify the functional groups present in the bacterial cell wall is Fourier Transform Infrared Spectroscopy (FT-IR). FT-IR spectrum of marine *Staphylococcus aureus* CASMTK1 in a range of 500–4000 cm^{-1} for the presence of band assignments (Supplementary Table S2) and functional groups, including 888-C-H Plane bending, 932-O-H bending, 1041-CO-O-CO stretching, 1075-C-O stretching, 1118-C-O stretching, 1238-C-N stretching, 1307-C-O stretching, 1402-S=O stretching, 1447-C-H bending, 1545-N-O bending, 1659-N-H bending, 2101-N=C=S stretching, 2849-C-H stretching, 2871-C-H stretching, 2926-C-H stretching, 2959-C-H stretching, 3435- O–H stretching, H–bonded are found in bacterial structural and functional groups were determined. Additionally *Staphylococcal hyaluronidase* enzyme

was revealed in a range of 1500–1700 cm^{-1} for the presence of the amide I as evident by six bands at 1636, 1647, 1653, 1662, 1669 and 1675 cm^{-1}; and Amide II by seven bands at 1516, 1521, 1533, 1540, 1559, 1570 and 1577 cm^{-1}. The band at 1516 cm^{-1} representing a tyrosine residue, was easily recognizable with the bands at 1585 and 1565 cm^{-1} which corresponded to absence of aspartate and much smaller amount of glutamate (Figure 6). The FTIR spectrum also revealed the inter molecular β-sheet and α-helix.

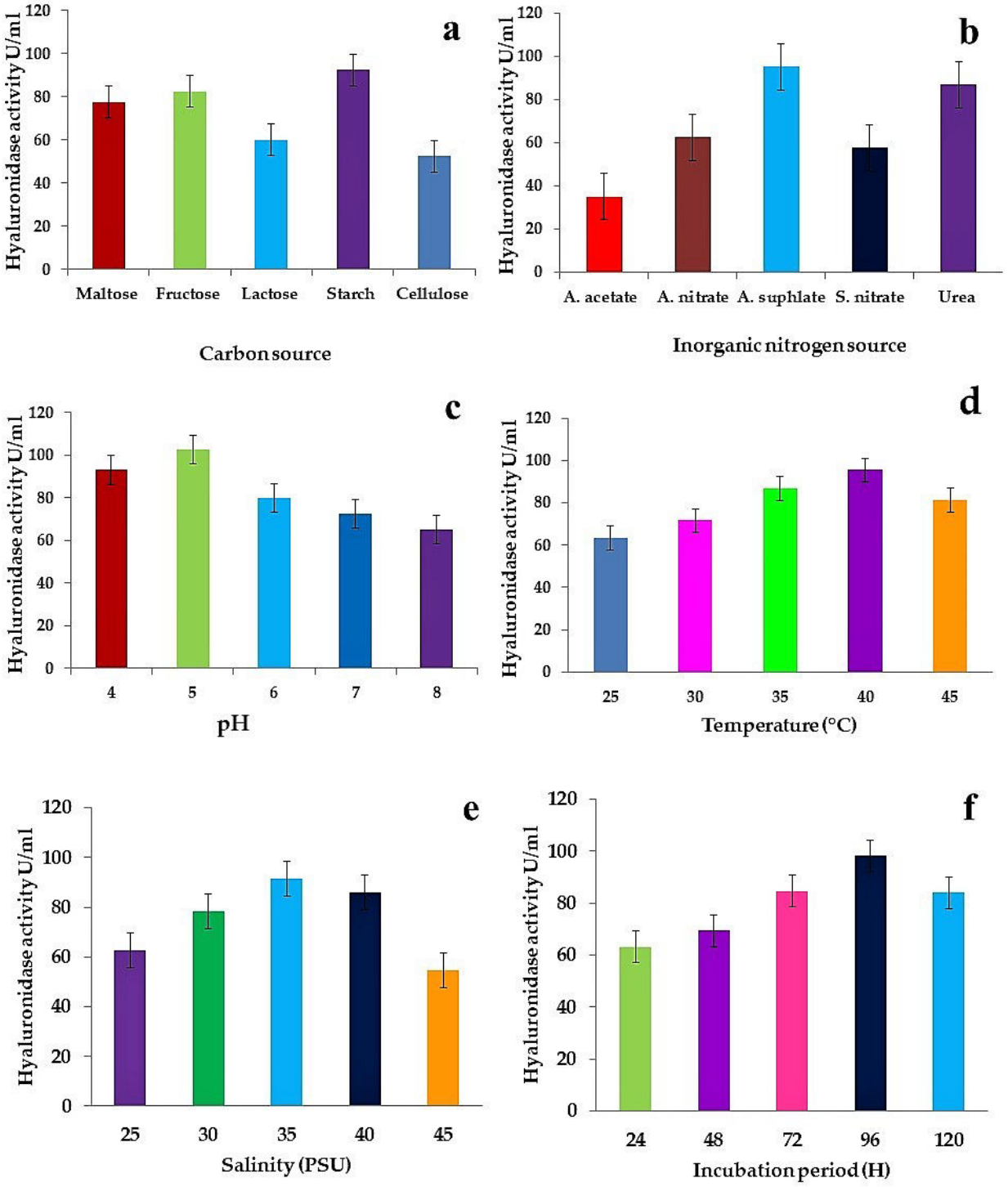

Figure 5. Optimization of hyaluronidase enzyme production from marine *S. aureus* CASMTK1. The optimization and production of hyaluronidase were done under nutritional factors and physical factors (**a**) carbon source, (**b**) inorganic nitrogen source, (**c**) pH (**d**) temperature (**e**) salinity (**f**) incubation period.

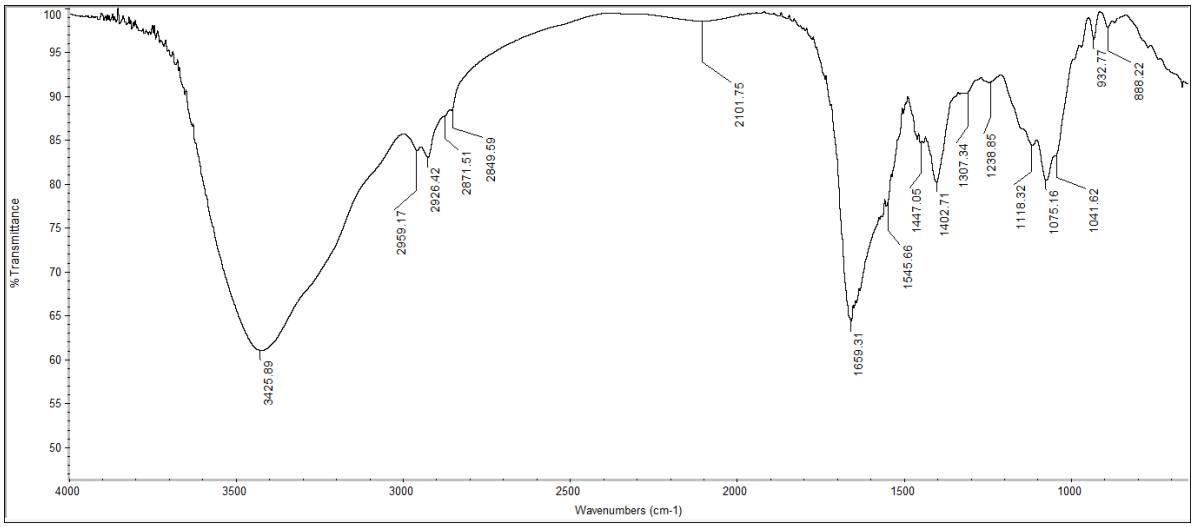

Figure 6. FT−IR spectroscopy spectrum of hyaluronidase enzyme. FTIR Band assignments of hyaluronidase in the region of 4000–500 cm^{-1}.

FTIR was compared with Raman Spectroscopy for CASMTK1 in a range of 500–3000 cm^{-1} for the presence of band assignments (Supplementary Table S3) and functional groups were 452-C-N-C Bend, 616-C=O Plane bend, 760-C-Cl stretch, 909-CH_2 Plane, 985-CH_2 Plane, 1057-S=O Stretch, 1184-C-O Stretch, 1293-C-F Stretch, 1399-COO- Carboxylic acid, 1466-CH_2 Scissors vibrations, 1707-C=O Stretch, 1996- Benzene Ring, 2091-C≡ stretch, 2763-NH stretching, 2815-CH stretching, 2950-CH stretching, 3050-H bonded OH stretch were found in bacterial structural, and the functional groups were determined. FT−IR and Raman spectral identification was determined for *Staphylococcus aureus* CASMTK1. Simultaneously bacterial strain in the presence of amide-II were evidenced by the three Raman shifts at 1526, 1541 and 1575 cm^{-1}. Where the primary Raman peaks at 1526 and 1541 cm^{-1} were due to N-H bending, while the secondary Raman peak at 1575 cm^{-1} was due to N-H bending. In addition, the Raman shift at 1689 cm^{-1} could be assigned to C=C stretching of amides (Figure 7).

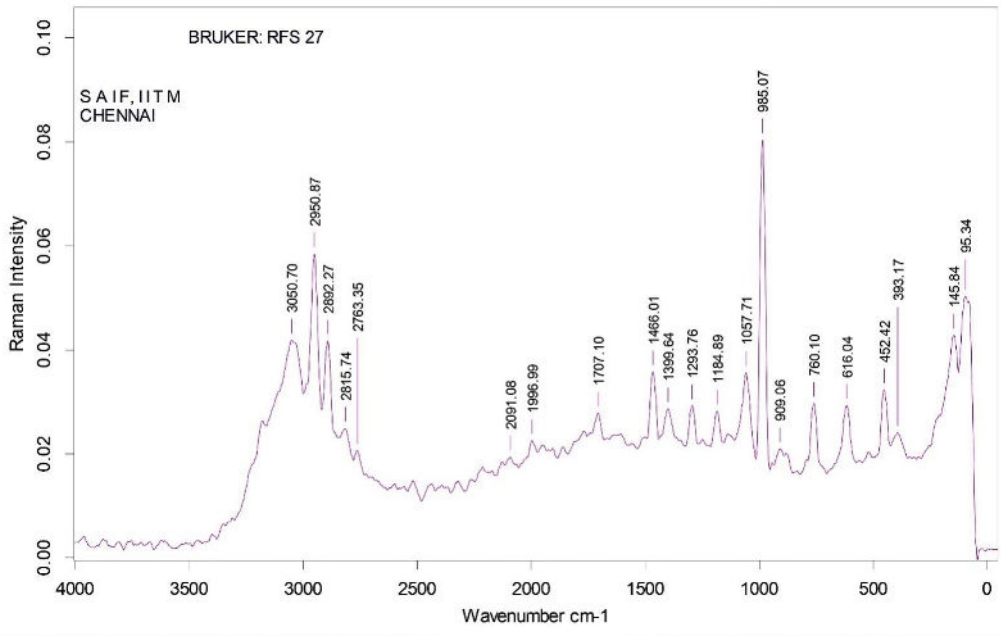

Figure 7. FT−R spectroscopy spectrum of hyaluronidase enzyme. FT Raman Band assignments of hyaluronidase in the region of 4000–500 cm^{-1}.

3.5. In-Vitro Antioxidant Properties

The total reducing power of staphylococcal hyaluronidase increased in a concentration dependent manner, and the reducing power at 10, 20, 30, 40 and 50 µg/mL was found to be 5, 15, 28, 43 and 65% respectively as compared to L-ascorbic acid as control. The decreasing power of the enzyme was less than that of reducing power of L-ascorbic acid. The enzyme exhibited maximum reducing power of 65% at the concentration of 50 µg/mL (Figure 8a). The total antioxidant activity of the enzyme increased with concentration. The total antioxidant activity of enzyme at different concentrations of 10, 20, 30, 40 and 50 µg/mL was found to be 9, 21, 39, 50 and 67% respectively as compared with L-ascorbic acid. The total antioxidant scavenging activity of enzyme was equal to that of L-ascorbic acid (Figure 8b).

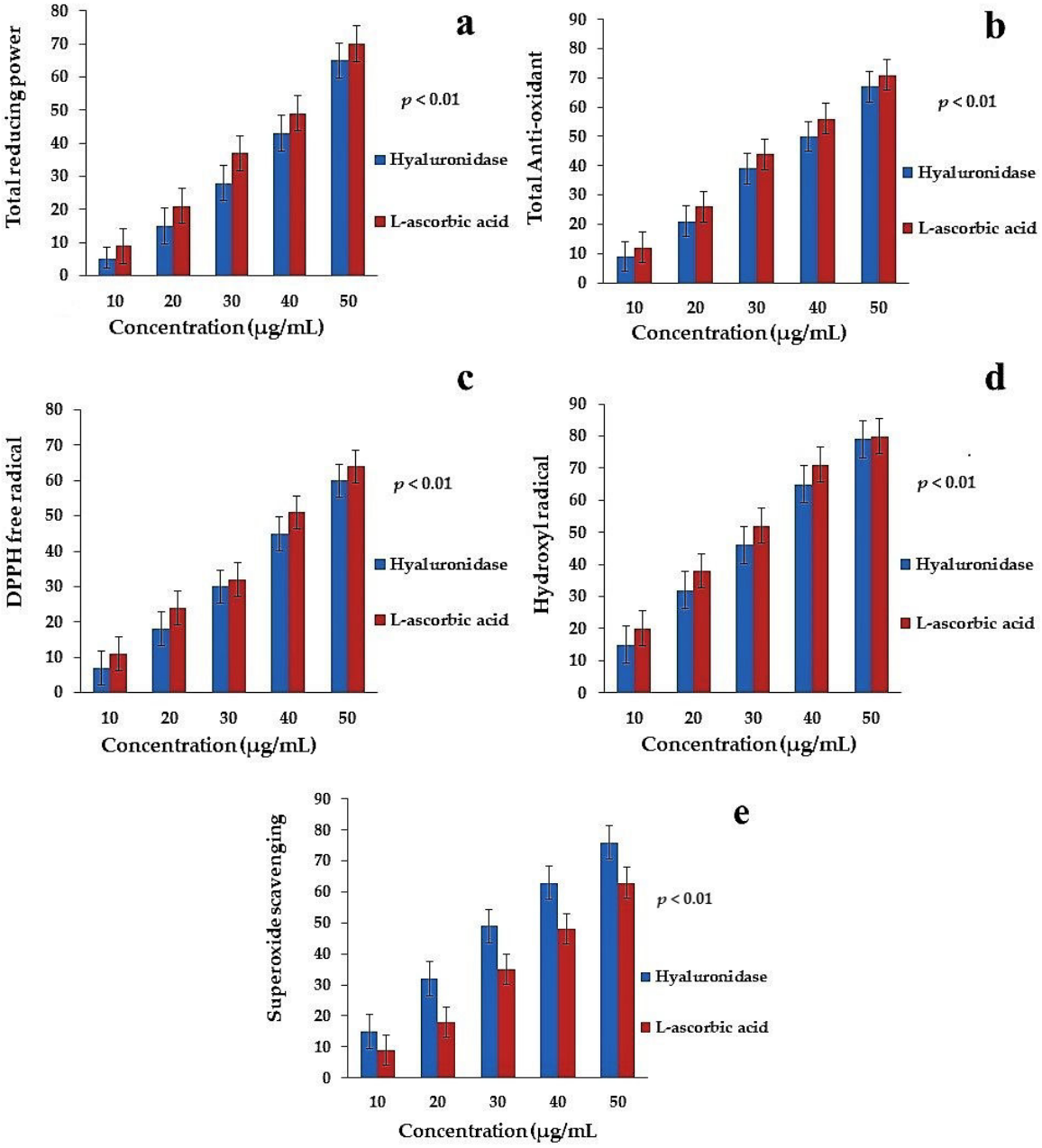

Figure 8. Antioxidant activity in different concentrations of hyaluronidase from CASMTK1, (**a**) reducing power, (**b**) total antioxidant, (**c**) DPPH scavenging, (**d**) Hydroxy radicals scavenging, (**e**) Superoxide scavenging.

The (DPPH) scavenging effect of hyaluronidase at 10, 20, 30, 40 and 50 µg/mL was found to be 7, 18, 27, 45 and 60% respectively. The potency of hyaluronidase to scavenge DPPH could also reflect its efficiency to inhibit the formation of free radicals (Figure 8c). The hydroxyl radical scavenging effect of enzyme at various concentrations of 10, 20, 30, 40 and 50 µg/mL was found to be 15, 32, 46, 65 and 79% respectively (Figure 8d). The superoxide anions scavenging activity of hyaluronidase at different concentrations of 10, 20, 30, 40 and 50 µg/mL was found to be 6, 32, 49, 63 and 76% respectively. (Figure 8e).

3.6. Effect of Staphylococcal Hyaluronidase on Cell Proliferation in MCF-7 Breast Cancer Cells (MTT Assay)

Staphylococcal hyaluronidase significantly inhibited proliferation of MCF-7 cells as determined by MTT assay. The Figure 9 reveals the changes in the percentage of cell viability in control and staphylococcal hyaluronidase treated in different concentrations ranged from 10 to 100 µg/mL in MCF-7 cells. In total, 100% of apoptosis was recorded at 80 µg/mL of enzyme in MCF-7 cells, hence the inhibitory concentration of hyaluronidase at which 50% MCF-7 cell death occurred (IC_{50}) was 40 µg/mL (Figure 9a) which was nearer to the effect of standard anticancer drug, paclitaxel.

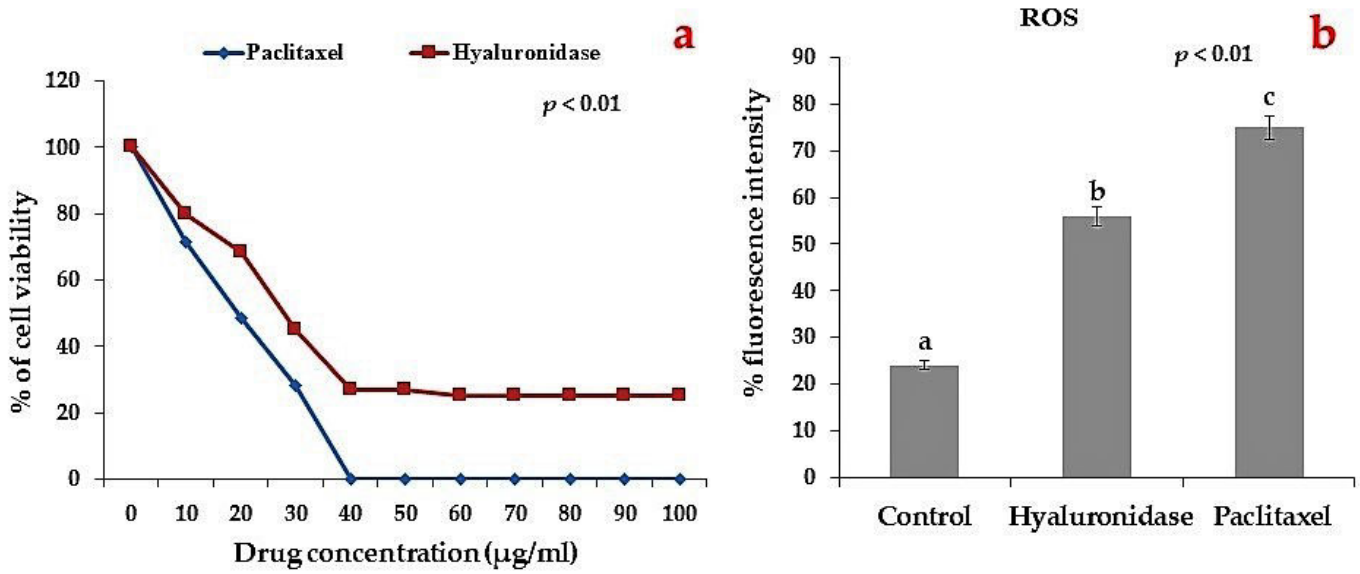

Figure 9. (**a**) Effect of Staphylococcal hyaluronidase on % of cell viability (24 h) in the control and enzyme-treated MCF-7 cells. IC_{50} value was plotted by taking the enzyme concentration on *x*-axis versus percentage of cell viability on *y*-axis. Values are given as mean ± S.D. of six experiments in each group. Values not sharing a common marking differ significantly at $p \leq 0.05$. (**b**) Effect of Staphylococcal hyaluronidase on ROS levels as measured By DCF fluorescence intensity using spectrofluorometer. Values are given as mean ± S.D. of six experiments in each group. Values not sharing a common marking (a–c) differ significantly at $p \leq 0.05$.

3.7. Effect of Staphylococcal Hyaluronidase on Intracellular ROS Levels in MCF-7 Cells

Figure 10a–c shows the fluorescence microscopic images which confirmed the low production of ROS in unprocessed MCF-7 cells. Staphylococcal hyaluronidase treatment showed enhanced ROS production in MCF-7 cells and the maximum generation of ROS in MCF-7 cells was nearer to the standard drug, paclitaxel.

3.8. Effect of Staphylococcal Hyaluronidase on Apoptotic Changes in MCF-7 Cells

Apoptotic morphological changes in different treatment groups are presented in Figure 11a–c. An apoptotic feature with condensed or fragmented chromatin, an indication of cell death, was observed in staphylococcal hyaluronidase-treated MCF-7 cells. Control cells showed equally distributed acridine orange stain (green fluorescence) with no

morphological changes whereas enzyme-treated cells exhibited apoptotic characteristics of membrane damage as evidenced by ethidium bromide fluorescence. Figure 11d shows the quantitative result of apoptosis in the different treatment groups of staphylococcus hyaluronidase treatment exhibiting 78% apoptotic cells.

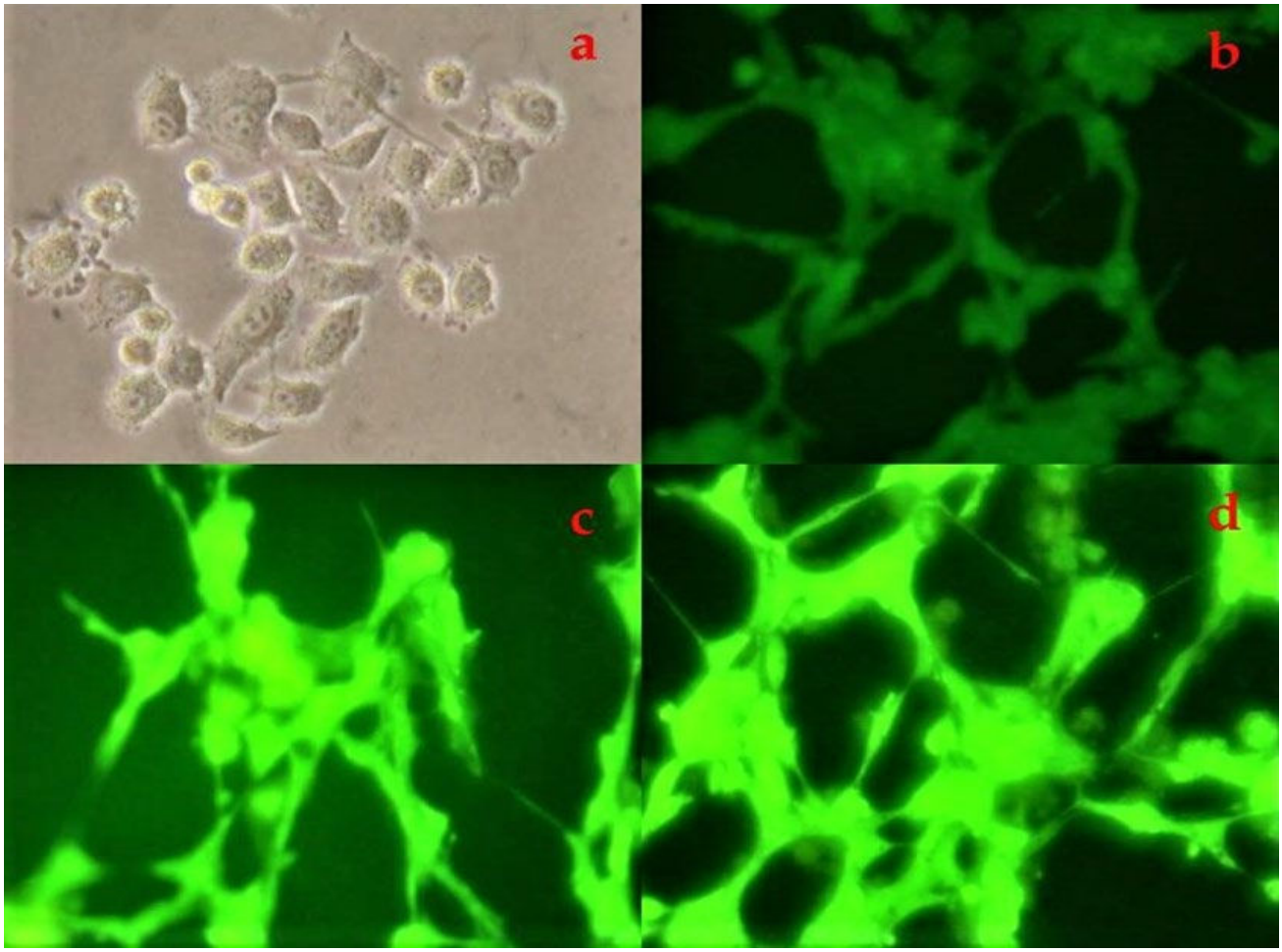

Figure 10. (**a**) Morphology of MCF-7 cancer cell line. (**b**) control, (**c**) Staphylococcal hyaluronidase treated cell. Proliferation of MCF-7 cells was significantly inhibited by Staphylococcal hyaluronidase. There was a 100% cell death at 80 µg/mL concentration of Staphylococcal hyaluronidase in MCF-7 cells. A 40 µg/mL of Staphylococcal hyaluronidase the anticancer activity was recorded without cell death. (**d**) Standard Paclitaxel treated. Microscopic images show the intracellular ROS in MCF-7 cells representing high DCF fluorescence. The maximum generation of ROS capacity of Staphylococcal hyaluronidase in MCF-7 was very nearer to the maximum generation of ROS capacity of standard drug paclitaxel.

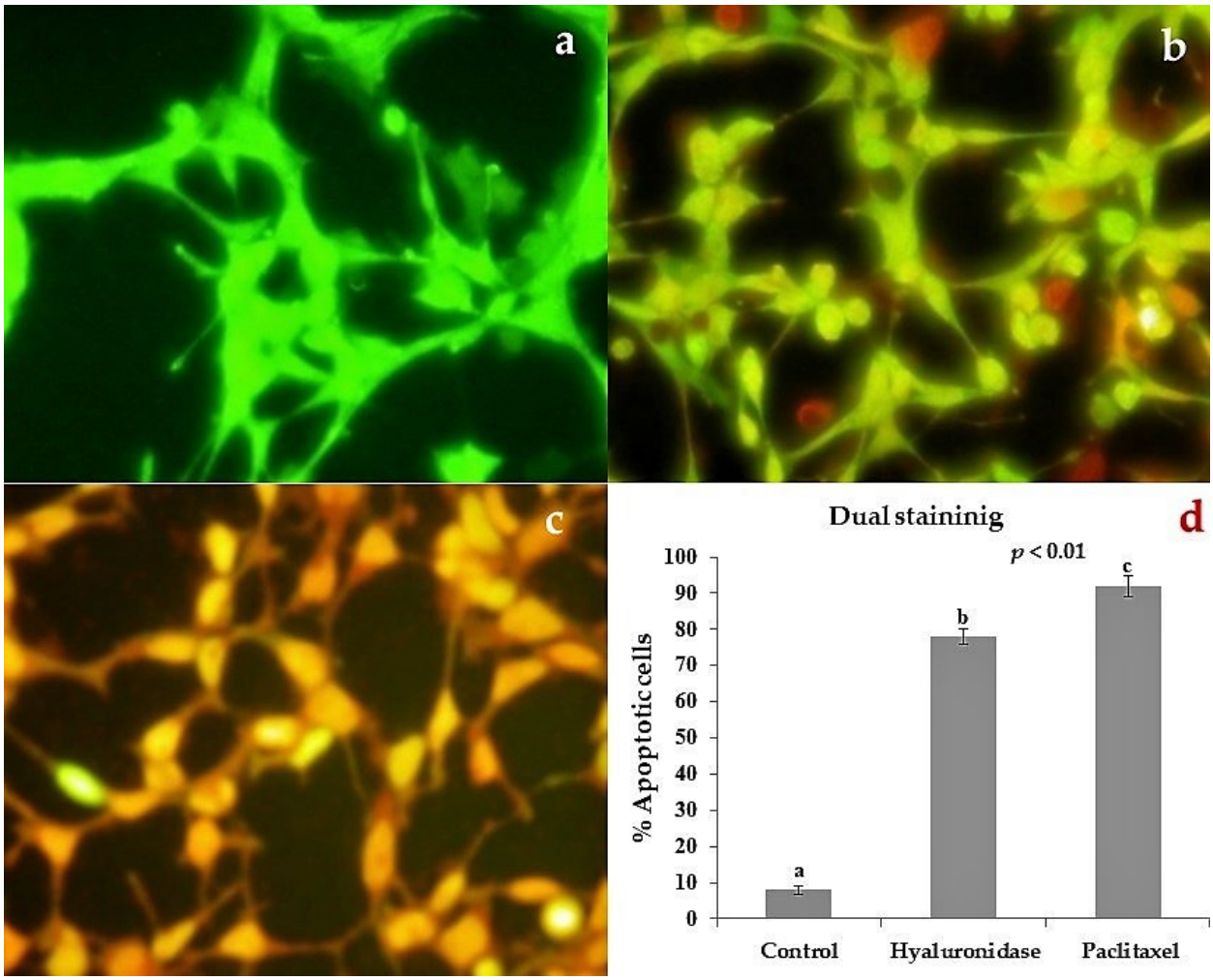

Figure 11. Microscopic image showing apoptotic morphological changes, as assessed by EtBr and AO staining. (**a**) control cells showed evenly distributed acridine orange stain (green fluorescence) with no morphological changes, (**b**) Staphylococcal hyaluronidase treated cells. The apoptotic features with condensed or fragmented chromatin were observed in Staphylococcal hyaluronidase treated MCF-7 cells, (**c**) Standard Paclitaxel treated cells showed apoptotic morphological features and cell damage. (**d**) Effect of Staphylococcal hyaluronidase on apoptosis (%) in MCF-7 cells. Values are given as mean ± S.D. of six experiments in each group. Values not sharing a common marking (a–c) differ significantly at $p \leq 0.05$.

4. Discussion

The present study isolated 12 strains of *Staphylococcus* sp., from coastal waters of Parangipettai in south-east coast of India as evident by traditional biochemical and microscopic techniques. Of the 12 isolates, CASMTK1 was found potential for the production of hyaluronidase, and it was further tested for molecular identification, antioxidant and antibreast cancer activities. Earlier studies reveal the occurrence of *Staphylococcus aureus* in unpolluted region of seawater from west side to east end of the earth as 5% from Narragansett Bay, Chesapeake Bay, and Atlantic Ocean coastal and open ocean waters east of cape Henry [41], as 9.3% from Japan, 20.4% from South China sea [42], 76.9% of surface water samples from Portugal [43] and as 98.1% from Hawai'i [44]. The present study examined *Staphylococcus* sp. (CASMTK1) by sequencing its 16S region of rRNA and the sequence had a high similarity to other *Staphylococcus* species sequences in GenBank data base. Phylogenetic study verified the relationship between the species of the genus *Staphylococcus*. The technique of 16S rRNA gene sequences for classifying and identi-

fying prokaryotes depends primarily on comparing the database of relevant species of known sequences in particular, sequences of typical strains of 99% of prokaryotic species with available NCBI databases [45]. In general, hyaluronidase producing bacteria belong to the genus of *Streptococcus*, *Streptomyces* and *Staphylococcus* [46]. The enzyme aids in invasion of bacteria by degrading hyaluronic acid-rich host tissue. Furthermore, the hyaluronan oligomers of the enzymes are powerful inflammatory agents that promote a microbial friendly environment [24]. Previous studies have investigated the presence of hyaluronidase in *Staphylococcus* species, and these species are also reported to be positive for coagulase and DNAase activities [47]. The present study also found the potential of marine *staphylococcus* species in production of hyaluronidase and also it was found to be influenced by carbon and inorganic nitrogen sources, pH, salinity, incubation period, and temperature.

The bacterial production of hyaluronidase increased with increasing salinity, and this high level of salt tolerance of the marine *Staphylococcus* species will be favourable for the industrial application. Consequently, there is a growing interest in using the marine bacteria for medical applications [48]. The carbon source is required for hyaluronidase production, whereas bacterial phosphotransferase system (PTS) transporters allow the uptake of sugars from the external surroundings, concomitant phosphorylation, and release into the cytoplasm as sugar-phosphates. The use of phosphoenolpyruvate (PEP) as phosphoryl donor and power source of *Staphylococcus aureus* has a completely unique PTS delivery system for N-acetylglucosamine [49]. Of the carbon sources tested, the maximum enzyme yield of 92.5 U/mL was in starch. Of inorganic nitrogen sources examined, the optimal enzyme production of 95.0 U/mL was in ammonium sulphate. The highest enzyme production was also achieved at pH 5 and 45 °C. Such optimization of hyaluronidase has already been made [50] as well in *Bacillus* species (CQMU-D, A50) [51], similar to the present study using marine *S. aureus.*

In the present work, the strain CASMTK1 with the highest specific activity of the hyaluronidase enzyme was 33.26% in ammonium sulphate precipitation, 24.12% in ion exchange chromatography and 18.36% in gel filtration chromatography. The partial purified Staphylococcal hyaluronidase showed the molecular weight of 92 kDa, which falls in the range of 50–160 kDa molecular weight as reported earlier for bacterial hyaluronidase [24,52]. These studies are mostly on hyaluronidase of low molecular weight; however, the high molecular weight hyaluronidase showed no significant homology with the low molecular weight hyaluronidase, proving its mechanism of degradation of hyaluronic acid [53]. The balance between the synthesis and degradation techniques of hyaluronic acid performs a crucial regulatory function in the human body, as it determines not solely the quantity of hyaluronic acid, but its molecular weight determines a number of organic actions of the hyaluronic acid [54]. The secondary structure of the hydrogen bonding is responsible for stiffness of the chain in hyaluronidase [55] in accordance with the present study as evident by FT-IR and FT-Raman spectroscopy. The IR absorption bands between about 4000 and 500 cm^{-1} are more often assigned to the functional groups. In addition, functional groups corresponding to the bands at 1113 cm^{-1}, 1077 cm^{-1}, 1025 cm^{-1} as well C-O stretching and C-1-H bending vibrations in sugars of recombinant hyaluronidase (*Apis mellifera* in *E. coli* B121 (DE3)) is identified in the FT-IR spectrum [56], which is in support of the present staphylococcal hyaluronidase. FTIR spectra were used in the present study to analyse the crude extract for the presence of functional chemical groups. This identified a typical amine group, protein methyl groups, lipid C-H stretching vibrations, a C-N group, an OH group of ribose rings, and carbohydrate C-OH groups, similar to earlier works [56].

Antioxidants play vital roles in the upkeep of cell integrity and accordingly are imperative in keeping the homeostasis of the host immune system. The stability between the ranges of pro-oxidants and antioxidants defines the cell destiny of genomic integrity by means of retaining the redox reputation of the cells. These antioxidants protect against cell damage by reacting and eliminating oxidizing free radicals, and this is relevant to adjuvant chemotherapy [57].

The present work revealed antioxidant activities for staphylococcal hyaluronidase by five different in-vitro assays. The ability of hyaluronidase to scavenge DPPH could also reflect its ability to inhibit the formation of free radicals. The presence of carboxylic groups in hyaluronidase is most likely responsible for its anti-radical properties [58]. This will be defined by fact that; the antioxidants donate protons to the loose radicals to neutralize rate within the solution as a result of which the absorbance decreases at wavelength at 515 nm [59]. Earlier work has found that low molecular weight hyaluronic acid degrades with the aid of hydroxyl radical as an antioxidant mechanism [60]. Superoxide anion is likewise known to initiate indirectly the fat peroxides as a result of the creation of H_2O_2 in generating hydroxyl radical [61]. Many researchers have reported on the ability of hyaluronic acid to chelate sundry ions and transition metals [58]. The hydroxy radical is the most harmful. ROS is especially responsible for oxidative damage to biomolecules. For example, superoxide anion radicals immediately initiate lipid peroxidation [61]. ABTS and DPPH radical scavenging techniques are the common spectrophotometry methods for the determination of the antioxidant activity. The ABTS radical cation creation takes place directly by the addition of potassium persulphate in ABTS solution. The present study determined the antioxidant capacity of hyaluronidase in-vitro at various doses on ABTS.

Our study revealed that Staphylococcal hyaluronidase increased the antioxidant properties of total reducing power, DPPH radical scavenging, total antioxidant, superoxide scavenging, in a dose dependently manner, similar to previous works [62–64]. In addition, Staphylococcal hyaluronidase enzyme was found to have carboxylic and hydroxylic functional groups, which enhanced the antioxidant properties. This is the first line of defence against the adverse effects of cell damage caused by free radicals, and it is essential to maintain optimal health through different mechanisms of action. The reactive oxygen species, especially hydroxyl and peroxyl radicals, hydrogen peroxide, and superoxide radical anions, have long been implicated in oxidative destruction of lipids, DNA, proteins, and other cellular components. Several reactive oxygen species are created from superoxide, including hydrogen peroxide (H_2O_2), peroxide anion, and hydroxyl radical (OH), and these are used by cells for differentiation, proliferation, apoptosis, migration, and contraction [65,66].

In the present study, the in-vitro anticancer properties of partially purified staphylococcal hyaluronidase were tested in the human breast cancer cell line (MCF-7) by MTT assay. The enzyme treatment significantly decreased the percentage of cell viability in MCF-7 cells with LC_{50} value of 40 µg/mL by inducing apoptosis of cancer cells. The drug dosage level lower than 30 µg/mL is much effective [67]. Therapeutic index value of hyaluronidase enzyme is calculated for the safety of the drug. Drugs are considered for further testing only when the therapeutic index value is 16 or above [63]. The present research work revealed a therapeutic index value of 18.48 for hyaluronidase enzyme against breast cancer. Hence, further purification of the enzyme will provide the most effective anticancer drug. In the current investigation, it was discovered that enzyme pre-treatment dramatically exacerbated morphological alterations associated with apoptosis in MCF-7 cells. The morphology of apoptosis in cells undergoing pyknosis, chromosomal condensation, and nuclear fragmentation were observed under a microscope in enzyme-treated cell at the dose of 40 µg/ml, and this treatment showed 80% apoptosis. Staphylococcus hyaluronidase causes cytotoxicity, by disrupting mitochondrial dehydrogenase activity inside the cancer cell [68].

The elevated molecular mass of hyaluronate inhibits cell growth. Additional, it is well known that hyaluronidase therapy stimulates the production of hyaluronic acid [69], which strongly inhibits cell proliferation through damaging DNA by helical strand breakage, DNA cross-linking, and proteins as induced by ROS, which are connected with cancer initiation and advancement. However sometimes, a paradox in organic systems is that ROS can induce apoptotic cell death, which is a vital advance in cancer therapeutics [70]. In the present study, the ROS levels were evaluated after 24 h of incubation with hyaluronidase. The escalated ROS level occurred after the treatment, perhaps because of its disturbance in

the oxidative imbalance in cancer cells. The interactions between tumor cells and fibroblasts of the host may be responsible for the elevated hyaluronate concentration in tumors. The hyaluronidase treatment of tumor cells seems to have induced an irreversible replacement in cell cycle kinetics. Hence, hyaluronidase has already been used in anticancer treatment as it is believed to make penetration easier and to lower interstitial fluid pressure, allowing anticancer medicines to reach cancerous cells [71]. A key tactic for cancer treatment could be the use of medications that target the mitochondria in tumor cells to start mitochondrial-activated apoptosis [72]. The present work proved that partially purified staphylococcal hyaluronidase from marine *Staphylococcus aureus* has effective anticancer activity, which will be helpful for the therapeutic, and pharmaceutical applications in the future.

5. Conclusions

The present study partially purified hyaluronidase from marine *Staphylococcus aureus* CASMTK1, and its potency was almost similar to that of standard anticancer chemotherapy tested in the present study. This study created a new option for treating cancer, and this pioneer work on marine hyaluronidase will serve as baseline data to further understand the molecular aspects and exact mechanisms of action by the marine hyaluronidase enzyme both by in-vitro and in-vivo studies.

Supplementary Materials: The following supporting information can be downloaded at: https://www.mdpi.com/article/10.3390/jmse11040778/s1, Table S1: Optimization of hyaluronidase enzyme production from marine *S. aureus* CASMTK1, Table S2: FTIR band assignments of hyaluronidase the region of 500–4000 cm^{-1} and Table S3: FT-Raman band assignments of hyaluronidase the region of 500–3000 cm^{-1}.

Author Contributions: K.T. and K.K. (Kalidasan Kaliyamoorthy) designed the study, performed the laboratory experiments, prepared the original draft, performed the data analysis, and completed the writing, review, and editing of the manuscript, K.K. (Kathiresan Kandasamy) and M.P. helped to design the study, reviewed, and edited the manuscript. V.V., S.C. and L.D. helped to design the study, wrote the methodology, reviewed, edited, and approved the manuscript. All authors have read and agreed to the published version of the manuscript.

Funding: This work was supported by Second Century Fund (C2F) Postdoctoral Scholarship of Chulalongkorn University, Thailand Science Research and Innovation Fund Chulalongkorn University (DIS66230010), NRCT-JSPS Core to Core Program, CREPSUM JPJSCCB20200009, National Research Council of Thailand and Chulalongkorn University (N42A650257), Thailand Science Research and Innovation Fund Chulalongkorn University (DIS66230006), and Busrakham Jasmine Limited. Busrakham Jasmine Limited was not involved in the study design, collection analysis, interpretation of data, the writing of this article or the decision to submit it for publication.

Institutional Review Board Statement: Not applicable.

Informed Consent Statement: Not applicable.

Data Availability Statement: Not applicable.

Acknowledgments: The authors are thankful to CAS in Marine Biology, Annamalai University for providing the necessary facilities, meticulous, untiring guidance, encouragement and motivation for this work. Laurent Dufossé thanks the Conseil Régional de Bretagne and the Conseil Régional de La Réunion for continuous financial support when developing research activities dedicated to microbial biotechnology.

Conflicts of Interest: The authors declare no conflict of interest.

References

1. World Health Organisation (WHO). International Statistical Classification of Tumors of the Breast. 2023. Available online: https://www.iarc.who.int (accessed on 26 December 2022).
2. Siegel, R.L.; Miller, K.D.; Fuchs, H.E.; Jemal, A. Cancer statistics, 2022. *CA Cancer J. Clin.* **2022**, *7*, 7–33. [CrossRef] [PubMed]
3. Renan, M.J. How many mutations are required for tumorigenesis? Implications from human cancer data. *Mol. Carcinog.* **1993**, *7*, 139–146. [CrossRef] [PubMed]

4. Al-Shamsi, H.O.; Abu-Gheida, I.H.; Iqbal, F.; Al-Awadhi, A. *Cancer in the Arab World*; Springer: Berlin/Heidelberg, Germany, 2022; p. 476. [CrossRef]
5. Torre, L.A.; Islami, F.; Siegel, R.L.; Ward, E.M.; Jemal, A. Global cancer in women: Burden and trends. *Cancer Epidemiol. Biomark. Prev.* **2017**, *26*, 444–457. [CrossRef] [PubMed]
6. Harbeck, N.; Penault-Llorca, F.; Cortes, J.; Gnant, M.; Houssami, N.; Poortmans, P.; Ruddy, K.; Tsang, J.; Cardoso, F. Brest Cancer. *Nat. Rev.* **2019**, *5*, 66. [CrossRef]
7. Waks, A.G.; Winer, E.P. Breast cancer treatment: A review. *J. Am. Med. Assoc.* **2019**, *321*, 288–300. [CrossRef]
8. Bedard, P.L.; Hyman, D.M.; Davids, M.S.; Siu, L.L. Small molecules, big impact: 20 years of targeted therapy in oncology. *Lancet* **2020**, *395*, 1078–1088. [CrossRef]
9. Bedard, P.L.; Piccat-Gebhart, M.J. Current paradigms for the use of HER2-Targeted therapy in early-stage breast cancer. *Clin. Breast Cancer* **2008**, *8*, 157–165. [CrossRef]
10. Bouris, P.; Skandalis, S.S.; Piperigkou, Z.; Afratis, N.; Karamanou, K.; Altras, A.J.; Moustakas, A.; Theocharis, A.D.; Karamanos, N.K. Estrogen receptor alpha mediates epithelial to mesenchymal transisition, expression of specific matrix effectors and functional properties of breast cancer cells. *Matrix Biol.* **2015**, *43*, 42–60. [CrossRef]
11. Piperigou, Z.; Bouris, P.; Onisto, M.; Franchi, M.; Kletsas, D.; Theocharis, A.D.; Karamanos, N.K. Estrogen receptor beta modulates breast cancer cells functional properties, signaling and expression of matrix molecules. *Matrix Biol.* **2016**, *56*, 4–23. [CrossRef]
12. Wilkes, G.M. Targeted therapy: Attacking cancer with molecular and immunological targeted agents. *Asia Pac. J. Oncol. Nurs.* **2018**, *5*, 137–155. [CrossRef]
13. Meiser, B.; Wong, W.K.T.; Peate, M.; Julian-Reynier, C.; Kirk, J.; Mitchell, G. Motivators and barriers of tamoxifen use as risk reducing medication amongst women at increased breast cancer risk: A systematic literature review. *Hered. Cancer Clin. Pract.* **2017**, *15*, 14. [CrossRef]
14. Cuzick, J.; Sestak, I.; Bonanni, B.; Costantino, J.P.; Cummings, S.; DeCensi, A.; Dowsett, M.; Forbes, J.F.; Ford, L.; LaCroix, A.Z.; et al. Selective oestrogen receptor modulators in prevention of breast cancer: An updated meta-analysis of individual participant data. *Lancet* **2013**, *25*, 1827–1834. [CrossRef]
15. Nazarali, S.A.; Narod, S.A. Tamoxifen for women at high risk of breast cancer. *Breast Cancer* **2014**, *6*, 29–36. [CrossRef]
16. Fabian, C.J. The What, Why and how of aromatase inhibitors: Hormonal agents for treatment and prevention of breast cancer. *Int. J. Clin. Pract.* **2007**, *61*, 2051–2063. [CrossRef]
17. Krens, S.D.; McLeod, H.L.; Hertz, L.D. Pharmacogenetics, enzyme probes and therapeutic drug monitoring as potential tools for individualizing taxane therapy. *Pharmacogenomics* **2013**, *14*, 555–574. [CrossRef]
18. Oun, R.; Moussa, Y.E.; Wheate, N.J. The side effects of platinum-based chemotherapy drugs: A review for chemists. *Dalt. Trans.* **2018**, *47*, 6645–6653. [CrossRef]
19. Anitha, P.; Bhargavi, J.; Sravani, B.; Aruna, B.; Ramkanth, S. Recent progress of dendrimers in drug delivery for cancer therapy. *Int. J. Appl. Pharm.* **2018**, *10*, 34–42. [CrossRef]
20. Afonso, V.; Champy, R.; Mitrovic, D.; Collin, P.; Lomri, A. Reactive oxygen species and superoxide dismutases: Role in joint diseases. *Jt. Bone Spine* **2007**, *74*, 324–329. [CrossRef]
21. Valko, M.; Leibfritz, D.; Moncol, J.; Cronin, M.T.; Maur, M.; Telser, J. Free radicals and antioxidants in normal physiological functions and human disease. *Int. J. Biochem. Cell Biol.* **2007**, *39*, 44–84. [CrossRef]
22. Ravikumar, S.; Kathiresan, K. *Marine Pharmacology*; School of Marine Sciences, Alagappa University: Karaikudi, India, 2010; p. 215.
23. Jung, H. Hyaluronidase: An overview of its properties, applications, and side effects. *Arch. Plast. Surg.* **2020**, *47*, 297–300. [CrossRef]
24. Hynes, W.L.; Walton, S. Hyaluronidase of Gram-Positive Bacteria. *FEMS Microbiol. Lett.* **2000**, *183*, 201–207. [CrossRef] [PubMed]
25. Weber, G.C.; Buhren, B.A.; Schrumpf, H.; Wohlrab, J.; Gerber, P.A. Clinical applications of hyaluronidase. *Adv. Exp. Med. Biol.* **2019**, *1148*, 255–277. [CrossRef]
26. Cavallini, M.; Gazzola, R.; Metalla, M. The role of hyaluronidase in the treatment of complications from hyaluronic acid dermal fillers. *Aesthetic Surg. J.* **2013**, *33*, 1167–1174. [CrossRef] [PubMed]
27. Kloos, W.E.; Schleifer, K.H. Genus IV. Staphylococcus. In *Bergey's Manual of Systematic Bacteriology*; Sneath, P.H.A., Mair, N.S., Sharpe, M.E., Holt, J.G., Eds.; Williams & Wilkins: Baltimore, MD, USA, 1986; Volume 2, pp. 1013–1035.
28. Zhang, K.; Jo-Ann, M.; Sameer, E.; Thomas, L.; John, M.C. Novel Multiplex PCR Assay for Characterization and Concomitant Subtyping of Staphylococcal Cassette Chromosome mec Types I to V in Methicillin-Resistant *Staphylococcus aureus*. *J. Clin. Microbiol.* **2005**, *43*, 5026–5033. [CrossRef] [PubMed]
29. Tamura, K.; Stecher, G.; Peterson, D.; Filipski, A.; Kumar, S. MEGA6: Molecular Evolutionary Genetics Analysis version 6.0. *Mol. Biol. Evol.* **2013**, *30*, 2725–2729. [CrossRef]
30. Tam, Y.C.; Chan, E.C.S. Modifications enhancing reproducibility and sensitivity in the turbidimetric assay of hyaluronidase. *J. Microbiol. Methods* **1983**, *1*, 255–266. [CrossRef]
31. Bradford, M.M. A Rapid and Sensitive Method for the Quantification of Microgram Quantities of Protein Utilizing the Principle of Protein Dye Binding. *Anal. Biochem.* **1976**, *72*, 248–254. [CrossRef]
32. Xie, J.; Rileya, C.; Kumar, M.; Chittura, K. FTIR/ATR study of protein adsorption and brushite transformation to hydroxyapatite. *Biomaterials* **2002**, *23*, 3609–3616. [CrossRef]

33. Oyaizu, M. Studies on Product of Browning Reaction Prepared from Glucose Amine. *Jpn. J. Nutr.* **1986**, *44*, 307–315. [CrossRef]
34. Mensor, L.L.; Menezes, F.S.; Leitao, G.G.; Reis, A.S.; Dos Santos, T.S.; Coube, C.S.; Leitao, S.G. Screening of Brazilian Plant Extracts for Antioxidant Activity by the Use of Dpph Free Radical Method. *Phytother. Res.* **2001**, *15*, 127–130. [CrossRef]
35. Miller, N.J.; Castelluccio, C.; Tijburg, L.; Rice-Evans, C. The Antioxidant Properties of Theaflavins and their Gallate Esters-Radical Scavengers or Metal Chelators. *FEBS Lett.* **1996**, *392*, 40–44. [CrossRef] [PubMed]
36. Nishikimi, M.; Appaji, N.; Yagi, K. The Occurrence of Superoxide Anion in the Reaction of Reduced Phenazine Methosulfate and Molecular Oxygen. *Biochem. Biophys. Res. Commun.* **1972**, *46*, 849–854. [CrossRef] [PubMed]
37. Halliwell, B.; Gutteridge, J.M.; Aruoma, O.I. The Deoxyribose Method: A Simple Test Tube Assay for Determination of Rate Constants for Reactions of Hydroxyl Radicals. *Anal. Biochem.* **1987**, *165*, 215–219. [CrossRef]
38. Mosmann, T. Rapid Colorimetric Assay for Cellular Growth and Survival, Application to Proliferation and Cytotoxicity Assays. *J. Immunol. Met.* **1983**, *65*, 55–63. [CrossRef] [PubMed]
39. Philipson, L.H.; Westley, J.; Schwartz, N. Effect of Hyaluronidase Treatment of Intact Cells on Hyaluronate Synthetase Activity. *Biochemistry* **1985**, *24*, 7899–7906. [CrossRef]
40. Lakshmi, S.; Dhanaya, G.S.; Joy, B.; Padmaja, G.; Remani, P. Inhibitory Effect of an Extract of Curcuma Zedoariae on human Cervical Carcinoma Cells. *Med. Chem. Res.* **2008**, *17*, 335–344. [CrossRef]
41. Gunn, B.A.; Colwell, R.R. Numerical Taxonomy of Staphylococci Isolated from the Marine Environment. *Int. J. Syst. Bacteriol.* **1983**, *33*, 751–759. [CrossRef]
42. Irina, A.B. Incidence and Characteristics of *Staphylococcus aureus* and *Listeria monocytogenes* from the Japan and South China seas. *Mar. Poll. Bull.* **2011**, *62*, 382–387. [CrossRef]
43. Silva, V.; Ferreira, E.; Manageiro, V.; Reis, L.; Tejedor-Junco, M.T.; Sampaio, A.; Capel, J.L.; Caniça, M.; Igrejas, G.; Poeta, P. Distribution and Clonal Diversity of Staphylococcus aureus and Other *Staphylococci* in Surface Waters: Detection of ST425-t742 and ST130-t843 mecC-Positive MRSA Strains. *Antibiotics* **2021**, *10*, 1416. [CrossRef]
44. Gerken, T.J.; Roberts, M.C.; Dykema, P.; Melly, G.; Lucas, D.; De Los Santos, V.; Gonzalez, J.; Butaye, P.; Wiegner, T.N. Environmental Surveillance and Characterization of Antibiotic Resistant *Staphylococcus aureus* at Coastal Beaches. *Antibiotics* **2021**, *10*, 980. [CrossRef]
45. Chun, J.; Rainey, F.A. Integrating genomics into the taxonomy and systematics of the Bacteria and Archaea. *Int. J. Syst. Evol. Microbiol.* **2014**, *64*, 316–324. [CrossRef]
46. Zhu, C.; Zhang, J.; Li, L.; Zhang, J.; Jiang, Y.; Shen, Z.; Guan, H.; Jiang, X. Purification and characterization of Hyaluronate Lyase from *Arthrobacter globiformis* A152. *Appl. Biochem. Biotechnol.* **2017**, *182*, 216–228. [CrossRef]
47. Essers, L.; Radebold, K. Rapid and reliable identification of *Staphylococcus aureus* by a latex agglutination test. *J. Clin. Microbiol.* **1980**, *12*, 641–643. [CrossRef]
48. Adingra, A.; Kouadio, A.N.; Ble, M.C.; Kouassi, A.M. Bacteriological Analysis of Surface Water Collected from the Grand-Lahou Lagoon, Cote Divoire. *Afr. J. Microbiol. Res.* **2012**, *6*, 3097–3105. [CrossRef]
49. Lengeler, J.W.; Jahreis, K. Bacterial PEP-dependent carbohydrate: Phosphotransferase systems couple sensing and global control mechanisms. *Contrib. Microbiol.* **2009**, *16*, 65–87. [CrossRef]
50. Sahoo, S.; Prasana, K.P.; Satya, R.M.; Anindita, N.; Poluri, E.; Sashi, K.D. Optimization of Some Physical and Nutritional Parameters for the Production of Hyaluronidase by Streptococcus equi SED 9. *Acta Pol. Pharm.* **2007**, *64*, 517–522.
51. Wang, L.; Liu, Q.; Hao, R.; Xiong, J.; Li, J.; Guo, Y.; He, L.; Tu, Z. Characterization of a Hyaluronidase-Producing *Bacillus* sp. CQMU-D Isolated from Soil. *Curr. Microbiol.* **2022**, *79*, 328. [CrossRef]
52. Sting, R.; Schaufuss, P.; Blobel, H. Isolation and characterization of hyaluronidases from *Streptococcus dysgalactiae*, *S. zooepidemicus* and *S. equi*. *Zentralbl. Bakteriol.* **1990**, *272*, 276–282. [CrossRef]
53. Sun, J.; Han, X.; Song, G.; Gong, Q.; Yu, W. Microbacterium Cloning, expression, and characterization of a new glycosamino-glycan lyase from sp. H14. *Mar. Drugs* **2019**, *17*, 681. [CrossRef]
54. Lee, S.Y.; Kang, M.S.; Jeong, W.Y.; Han, D.W.; Kim, K.S. Hyaluronic acid based theranostic nanomedicines for targeted cancer therapy. *Cancers* **2020**, *12*, 940. [CrossRef]
55. Jamal, A.A.; Yahya, M.; Dieter, S.; Siegfried, W.; Reinhard, N. Characterization of Enzymatically Digested Hyaluronic Acid Using NMR, Raman, IR, and UV/Vis spectroscopies. *J. Pharm. Biomed. Anal.* **2003**, *31*, 545–550. [CrossRef]
56. Schwaighofer, A.; Ablasser, S.; Lux, L.; Kopp, J.; Herwig, C.; Spadiut, O.; Lendl, B.; Slouka, C. Production of Active Recombinant Hyaluronidase Inclusion Bodies from *Apis mellifera* in *E. coli* Bl21(DE3) and characterization by FT-IR Spectroscopy. *Int. J. Mol. Sci.* **2020**, *21*, 3881. [CrossRef] [PubMed]
57. Campo, G.M.; Avenoso, A.; Campo, S.; D'Ascola, A.; Ferlazzo, A.M.; Calatroni, A. The antioxidant and antifibrogenic effects of the glycosaminoglycans hyaluronic acid and chondroitin-4-sulphate in a subchronic rat model of carbon tetrachloride-induced liver fibrogenesis. *Chem. Biol. Interact.* **2004**, *148*, 125–138. [CrossRef] [PubMed]
58. Chunlin, K.; Lanping, S.; Deliang, Q.; Di, W.; Xiaoxiong, Z. Antioxidant activity of low molecular weight hyaluronic acid. *Food Chem. Toxicol.* **2011**, *49*, 2670–2675. [CrossRef]
59. Krasin' ski, R.; Tchórzewski, H.; Lewkowicz, P. Antioxidant effect of hyaluronan on polymorphonuclear leukocyte-derived reactive oxygen species is dependent on its molecular weight and concentration and mainly involves the extracellular space. *Postep. Hig. Med. Dosw.* **2009**, *63*, 205–212.

60. Mercê, A.L.R.; Marques Carrera, L.C.; Santos Romanholi, L.K.; Lobo Recio, M.Á. Aqueous and solid complexes of iron (III) with hyaluronic acid: Potentiometric titrations and infrared spectroscopy studies. *J. Inorg. Biochem.* **2002**, *89*, 212–218. [CrossRef]
61. Suffness, M.; Pezzuto, J.M. Assays related to cancer drug discovery. In *Methods in Plant Biochemistry: Assays for Bioactivity*; Hostettmann, K., Ed.; Academic Press: London, UK, 1990; Volume 6, pp. 71–133.
62. Kalidasan, K.; Asmathunisha, N.; Gomathi, V.; Dufossé, L.; Kathiresan, K. Isolation and Optimization of Culture Conditions of *Thraustochytrium kinnei* for Biomass Production, Nanoparticle Synthesis, Antioxidant and Antimicrobial Activities. *J. Mar. Sci. Eng.* **2021**, *9*, 678. [CrossRef]
63. Kalidasan, K.; Dufossé, L.; Manivel, G.; Senthilraja, P.; Kathiresan, K. Antioxidant and Anti-Colorectal Cancer Properties in Methanolic Extract of Mangrove-Derived *Schizochytrium* sp. *J. Mar. Sci. Eng.* **2022**, *10*, 431. [CrossRef]
64. Kalidasan, K.; Ravi, V.; Sunil, K.S.; Maheshwaran, M.L.; Kathiresan, K. Antimicrobial and anticoagulant activities of the spine of stingray *Himantura imbricate*. *J. Coast. Life Med.* **2014**, *2*, 89–93.
65. Roy, S.; Khanna, S.; Nallu, K.; Hunt, T.K.; Sen, C.K. Dermal wound healing is subject to redox control. *Mol. Ther.* **2006**, *13*, 211–220. [CrossRef]
66. Rathore, R.; Zheng, Y.M.; Niu, C.F.; Liu, Q.H.; Korde, A.; Ho, Y.S.; Wang, Y.X. Hypoxia activates NADPH oxidase ot increase (ROS)I and (Ca2+)I through the mitochondrial ros-pkcepsilon signaling axis in pulmonary artery smooth muscle cells. *Free Radic. Biol. Med.* **2008**, *45*, 1223–1231. [CrossRef]
67. Larnier, C.; Kerneur, C.; Robert, L.; Moczar, M. Effect of Testicular Hyaluronidase on Hyaluronate Synthesis by Human Skin Fibroblasts in Culture. *Biochim. Biophys. Acta* **1989**, *1014*, 145–152. [CrossRef]
68. Spruss, T.; Bernhardt, G.; Schonenberger, H.; Schiess, W. Hyaluronidase Significantly Enhances the Efficacy of Regional Vinblastine Chemotherapy of Malignant Melanoma. *J. Cancer Res. Clin. Oncol.* **1995**, *121*, 193–202. [CrossRef]
69. Baumgartner, G.; Gomar-Hoss, C.; Sakr, L.; Ulsperger, E.; Wogritsch, C. The Impact of Extracellular Matrix on the Chemoresistance of Solid Tumors Experimental Clinical Results of Hyaluronidase as Additive to Cytostatic Chemotherapy. *Cancer Lett.* **1998**, *131*, 85–99. [CrossRef]
70. Fallacara, A.; Baldini, E.; Manfredini, S.; Vertuani, S. Hyaluronic acid in the third Millennium. *Polymers* **2018**, *10*, 701. [CrossRef]
71. Brekken, C.; Bruland, O.S.; De Lange Davies, C. Interstitial fluid Pressure in Human Osteosarcoma Xenografts, significance of Implantation site and the Response to Intratum-oral Injection of Hyaluronidase. *Anticancer Res.* **2000**, *20*, 3503–3512.
72. Surh, Y.J. Cancer Chemoprevention with Dietary Phytochemicals. *Nat. Rev.* **2003**, *3*, 768–780. [CrossRef]